

# Nucleocytoplasmic Partitioning of the Plant Photoreceptors Phytochrome A, B, C, D, and E Is Regulated Differentially by Light and Exhibits a Diurnal Rhythm

Stefan Kircher,<sup>a</sup> Patricia Gil,<sup>a</sup> László Kozma-Bognár,<sup>b</sup> Erzsébet Fejes,<sup>b</sup> Volker Speth,<sup>a</sup>  
Tania Husselstein-Muller,<sup>a</sup> Diana Bauer,<sup>a</sup> Éva Ádám,<sup>b</sup> Eberhard Schäfer,<sup>a,1</sup> and Ferenc Nagy<sup>a,b,c,1</sup>

<sup>a</sup> Albert-Ludwigs-Universität Freiburg, Institut für Biologie II/Botanik, Schänzlestrasse 1, 79104 Freiburg, Germany

<sup>b</sup> Institute of Plant Biology, Biological Research Centre, Temesvári krt 62, H-6726 Szeged, Hungary

<sup>c</sup> Institute of Plant Biology, Agricultural Biotechnological Centre, Szent-Györgyi A 4, H-2101 Godollo, Hungary

**The phytochrome family of plant photoreceptors has a central role in the adaptation of plant development to changes in ambient light conditions. The individual phytochrome species regulate different or partly overlapping physiological responses. We generated transgenic Arabidopsis plants expressing phytochrome A to E:green fluorescent protein (GFP) fusion proteins to assess the biological role of intracellular compartmentation of these photoreceptors in light-regulated signaling. We show that all phytochrome:GFP fusion proteins were imported into the nuclei. Translocation of these photoreceptors into the nuclei was regulated differentially by light. Light-induced accumulation of phytochrome species in the nuclei resulted in the formation of speckles. The appearance of these nuclear structures exhibited distinctly different kinetics, wavelengths, and fluence dependence and was regulated by a diurnal rhythm. Furthermore, we demonstrate that the import of mutant phytochrome B:GFP and phytochrome A:GFP fusion proteins, shown to be defective in signaling in vivo, is regulated by light but is not accompanied by the formation of speckles. These results suggest that (1) the differential regulation of the translocation of phytochrome A to E into nuclei plays a role in the specification of functions, and (2) the appearance of speckles is a functional feature of phytochrome-regulated signaling.**

## INTRODUCTION

The survival of plants is determined by their competence to initiate adaptive growth and development in response to changes in the environment. Light is one of the most variable and essential environmental parameters. To monitor light quality, quantity, and direction, several photoreceptor systems have evolved in higher plants. Phytochromes are red/far-red light photoreversible pigments ideally fit for monitoring both the quality and quantity of light. Phytochromes control plant growth and development throughout the plant life cycle and can adjust developmental strategies corresponding to changes in the light environment (for reviews, see Kendrick and Kronenberg, 1994).

In higher plants, phytochromes are encoded by small gene families; in Arabidopsis, five genes, *PHYTOCHROME A* to *PHYTOCHROME E* (*PHYA* to *PHYE*), have been identi-

fied (Sharrock and Quail, 1989; Clack et al., 1994). It is believed that all five phytochrome genes code for functional photoreceptors (phyA to phyE, respectively) that are synthesized in the dark in their inactive Pr form. After red light (R) treatment, Pr is photoconverted to the active Pfr form, which can be converted back to Pr after far-red light (FR) absorption. Recently, phyA, -B, -C, and -E were expressed in yeast, and after chromophore assembly, the photoreversibility of reconstituted photoreceptors was demonstrated (Eichenberg et al., 2000). The observed differences in the spectral properties indicate that the various phytochrome species have distinct roles in monitoring variations in the light quality of the natural environment.

It has been demonstrated by several research groups that this strong diversity of phytochrome photosensory functions is reflected in multiple response modes. The ultimate physiological functions of the different phytochromes have been analyzed using photoreceptor mutants in Arabidopsis (for review, see Whitelam and Devlin, 1997).

PhyA, the most abundant phytochrome, controls the very-low-fluence-rate responses and the FR high-irradiance responses (Furuya and Schäfer, 1996). These two response types are essential for the induction of seed germination

<sup>1</sup> To whom correspondence should be addressed. E-mail schaege@ruf.uni-freiburg.de; fax 49-761-2032629 or e-mail nagyf@nucleus.szbk.u-szeged.hu; fax 36-62-433434.

Article, publication date, and citation information can be found at www.plantcell.org/cgi/doi/10.1105/tpc.001156.

and for the adaptation of seedling growth to dense shade (Shinomura et al., 1996). These response modes are in good agreement with the fact that phyA is very labile in its Pfr form. By contrast, phyB is stable and operates in the low-fluence-rate response mode and continuous R.

The low-fluence-rate response mode is characterized by R pulse inducibility and FR pulse-driven reversibility (Furuya and Schäfer, 1996). Thus, phyB can control germination, deetiolation of seedlings, and several responses during plant development (Koornneef et al., 1980; Robson et al., 1993; Botto et al., 1995; Devlin et al., 1996). PhyD and phyE also are believed to be light stable and were shown to influence internode elongation and flowering time in mature plants (Devlin et al., 1998, 1999). The physiological role of phyC is not yet defined because no phyC mutants have been isolated.

Characterization of constitutive photomorphogenic (COP)/DEETIOLATED mutants revealed that the switch between photomorphogenesis and etiolation also is regulated by a complex suppressor system that, in contrast to photoreceptors, promotes the etiolation pathway by repressing photomorphogenesis in darkness. Considering genetic, physiological, and molecular aspects, the best characterized among these mutants is COP1, which was identified a decade ago (Deng et al., 1991). Osterlund et al. (2000) provided evidence that COP1 regulates the degradation of HY5 (Oyama et al., 1997), a positively acting factor of light signaling cascades, by targeting this protein to the 26S proteasome.

Based on a series of other observations, it is now accepted that COP1 probably acts like an E3 ubiquitin-protein ligase by recruiting the ubiquitin-conjugating enzyme E2 and mediating the transfer of polyubiquitin from E2 to target proteins. Moreover, Wang et al. (2001) demonstrated that both photoactivated cryptochromes repress COP1 activity through direct protein-protein contact. Therefore, it was concluded that this direct regulation is primarily responsible for the cryptochrome-mediated blue light regulation of photomorphogenesis in Arabidopsis. In contrast to blue light, the exact role of COP1 in regulating phytochrome-mediated photomorphogenic development is not yet understood.

Our knowledge of the molecular mechanisms that mediate different response modes of the different phytochromes also is fairly limited. However, recent results have changed our view dramatically regarding the molecular nature of the signaling cascade required for phyA- and phyB-controlled responses. First, it has been shown that the subcellular partitioning of phyB is regulated by light (Sakamoto and Nagatani, 1996; Kircher et al., 1999; Yamaguchi et al., 1999). Nuclear localization of phyB:green fluorescent protein (GFP) is controlled by the R/FR reversible low-fluence-rate response mode (Kircher et al., 1999) and exhibits a characteristic fluence rate dependence (Gil et al., 2000). By contrast, nuclear import of phyA:GFP, which complements Arabidopsis mutants lacking functional phyA, is regulated by the very-low-fluence-rate and R/FR high-irradiance responses of phyA (Kim et al., 2000). Thus, the nuclear import of both

phyB:GFP and phyA:GFP show the basic characteristics of the well-described phyB and phyA modes of function, and these correlations suggest that the nuclear import of phytochromes is a major regulatory step in light-induced signaling (Nagy and Schäfer, 2000).

In parallel, phyA and phyB were shown to interact with the transcription factor-like protein PIF3 in yeast (Ni et al., 1998) in a conformation-dependent manner (Ni et al., 1999). More recently, Martinez-Garcia et al. (2000) demonstrated that PIF3 binds to various G-box sequences shown to be required for the light-induced expression of several genes (Menkens et al., 1995; Ishige et al., 1999). The reversible interaction of phyB with PIF3 is maintained when PIF3 is bound to the promoter of the CCA-1 gene, whose activity is required for phytochrome-regulated CAB gene expression and/or for a functional circadian clockwork (Wang et al., 1997; Schaffer et al., 1998; Wang and Tobin, 1998). Together, these data suggest that phyB localized in the nucleus functions as an integral light-adjustable component of transcriptional regulator complexes (Martinez-Garcia et al., 2000). This model is further confirmed by the fact that mutant derivatives of phyB, which have been shown to be defective in light signaling *in vivo*, exhibited a strongly reduced capability to interact with PIF3 *in vitro* (Ni et al., 1999).

Here, we show that phyC:GFP, phyD:GFP, and phyE:GFP fusion proteins, like phyA:GFP and phyB:GFP, are imported into the nuclei and form speckles. Analysis of transgenic plants made feasible the determination of the different light conditions that control the nucleocytoplasmic partitioning of these photoreceptors. In addition, we show that this process is regulated by a diurnal rhythm and that light-induced speckle formation by phyA:GFP and phyB:GFP in the nuclei shows a close correlation with the functionality of these photoreceptors in light-dependent signaling.

## RESULTS

### Expression of the phyA to phyE:GFP Fusion Proteins in Transgenic Plants

Transgenic Arabidopsis plants were generated via *Agrobacterium tumefaciens*-mediated transformation and expressed the Arabidopsis *PHYA* to *PHYE* cDNAs fused to the modified GFP4 (mGFP4) (Haseloff et al., 1997) reporter gene (Figure 1A). The expression of these transgenes was driven by the 35S promoter of *Cauliflower mosaic virus* (Benfey et al., 1990). For each construct, ~20 to 25 independent transgenic lines were generated. Hygromycin-resistant plantlets were transferred to the greenhouse, grown to maturation, and selfed. Homozygous progeny were selected for further studies either by observing the characteristic overexpression phenotypes (phyA and phyB) or by confirming the expression of the phy:GFP fusion proteins by protein gel blot analysis using specific antibodies and/or GFP and by microscopy.

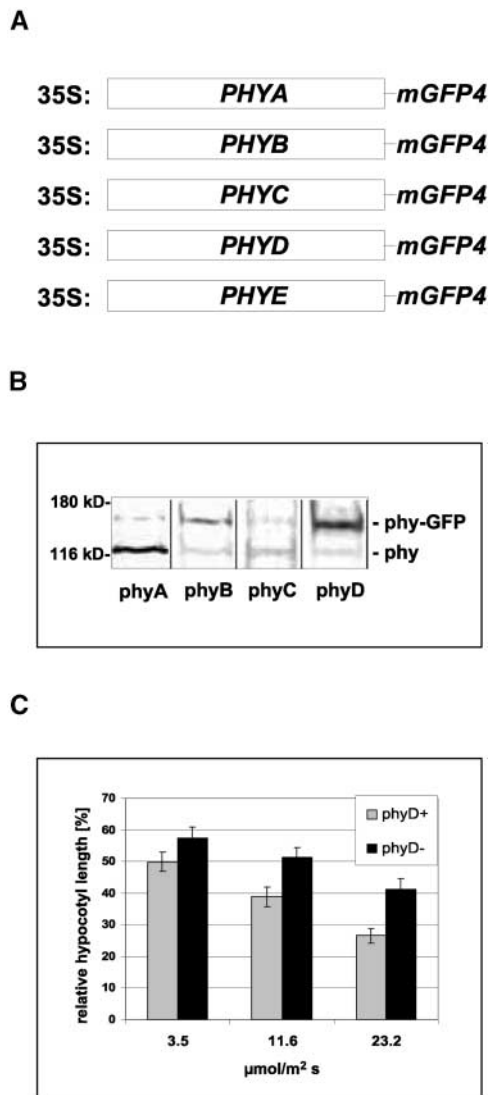


**Figure 1.** Construction and Expression of the 35S:PHYA to 35S:PHYE:mGFP4 Chimeric Genes in Transgenic Arabidopsis Plants.

**(A)** Diagrams of the Arabidopsis *PHYA*, *PHYB*, *PHYC*, *PHYD*, and *PHYE:mGFP4* gene fusions. Expression of these chimeric genes was driven by the 35S promoter of *Cauliflower mosaic virus*.

**(B)** Protein gel blot analysis of crude extracts for the detection of phyA to phyD:GFP fusion proteins in transgenic Arabidopsis plants. Total protein extracts were isolated from 7-day-old etiolated transgenic seedlings. Extracts then were subjected to SDS-PAGE and transferred subsequently to a polyvinylidene difluoride membrane. The ratios between endogenous phyA to phyD and phyA to phyD:GFP fusion proteins were determined using specific monoclonal antibodies.

**(C)** Ectopic overexpression of the phyD:GFP fusion protein modifies the phenotype of the *PHYD*-lacking Wassilewskija ecotype. Relative hypocotyl lengths in continuous R versus dark controls in *PHYD*-lacking (phyD<sup>-</sup>) and phyD:GFP-expressing (phyD<sup>+</sup>) seedlings are shown.

Protein gel blot analysis indicated that phyA to phyD:GFP fusion proteins were expressed and detected as ~145-kD protein bands using monoclonal antibodies specific for phyA to phyD (Figure 1B). This figure also shows the overexpression levels of the phyA to phyD:GFP fusion proteins (the ratios between endogenous phyA to phyD [ $\sim$ 120 kD] and the phyA to phyD:GFP fusion proteins [ $\sim$ 140 kD]) in the transgenic Arabidopsis lines selected for detailed studies. PhyA:GFP represented  $\sim$ 25% of the endogenous phyA, the amounts of the phyB:GFP and phyC:GFP fusion proteins were nearly identical to those of phyB and phyC, and phyD:GFP was overexpressed approximately fourfold. The overexpression level of phyE:GFP was not measured because of the low specificity of the antibody available to us.

Independent of the expression levels of the various phy:GFP fusion proteins, protein gel blot analysis indicated, using antibodies specific against GFP, that the phyA to phyD:GFP fusion proteins were not processed or degraded, because no low molecular mass products containing intact or degraded GFP were detected (data not shown). To determine the subcellular localization of the various phy:GFP fusion proteins, we analyzed at least 10 independent transgenic lines for each transgene. The expression levels of the particular phy:GFP fusion proteins generally varied not more than fivefold among those lines in which we could detect GFP fluorescence. The pattern of subcellular distribution of any phy:GFP fusion protein investigated in this study did not differ significantly among these plants. This finding indicates that the variability in the ratio of endogenous-to-recombinant phytochrome proteins, within this fivefold range, did not affect the nucleocytoplasmic distribution of the given fusion proteins discussed below.

It was reported recently that the phyA:GFP (Kim et al., 2000) and phyB:GFP (Yamaguchi et al., 1999; Gil et al., 2000) fusion proteins function as biologically active photoreceptors. Here, we demonstrate that ectopic expression of phyD:GFP complements the *PHYD* null mutant (i.e., it affects hypocotyl elongation in continuous R, as described in Aukerman et al. [1997]) (Figure 1C). Together, these data suggest that all phy:GFP fusion proteins, including phyE:GFP and phyC:GFP, represent functional photoreceptors.

To determine the nucleocytoplasmic distribution pattern of the various phy:GFP fusion proteins, homozygous progeny of primary transgenic plants analyzed by protein gel blotting, as described above, were grown under different light conditions. The localization of GFP was monitored by fluorescence microscopy as described in Kircher et al. (1999).

### Nuclear Import and Speckle Formation of the phyA to phyE:GFP Fusion Proteins Are Induced Differentially by Light

We determined the subcellular localization of the phyA to phyE:GFP fusion proteins in 7-day-old Arabidopsis seedlings germinated and grown as follows. Transgenic seeds

were allowed to imbibe in water for 48 h at 4°C in darkness. Then, they were irradiated with 18 h of white light (WL) to induce homogeneous germination, transferred back to darkness at 25°C, and grown for an additional 4 days.

Figures 2A and 2C show that phyA:GFP was not detectable in the nuclei in these seedlings. Import of the phyA:GFP fusion protein into the nuclei was induced by either WL or FR irradiations. After WL treatment, the accumulation occurred very fast—within minutes—accompanied by speckle formation in the nuclei and occasionally in the cytosol. Accumulation of phyA in the nuclei reached its maximum level after 10 min, which was followed by a rapid decline (Figures 2B and 3A).

The rapid loss of the nucleus-localized speckles and diffuse staining in WL is in good agreement with previous data showing the depletion of immunodetectable phyA:GFP fusion protein as a result of the degradation of phyA:GFP in its Pfr form (Kim et al., 2000). Irradiation with continuous FR also promoted the translocation of phyA:GFP and led to a very rapid appearance of phyA:GFP-containing speckles in the nuclei. The accumulation of phyA:GFP in the nuclei in continuous FR reached a maximum level in ~2 h (Figures 2D and 3B).

In the majority of 7-day-old dark-grown seedlings germinated after an inductive light treatment, phyB:GFP was localized in the cytosol (Figure 2E). However, in contrast to

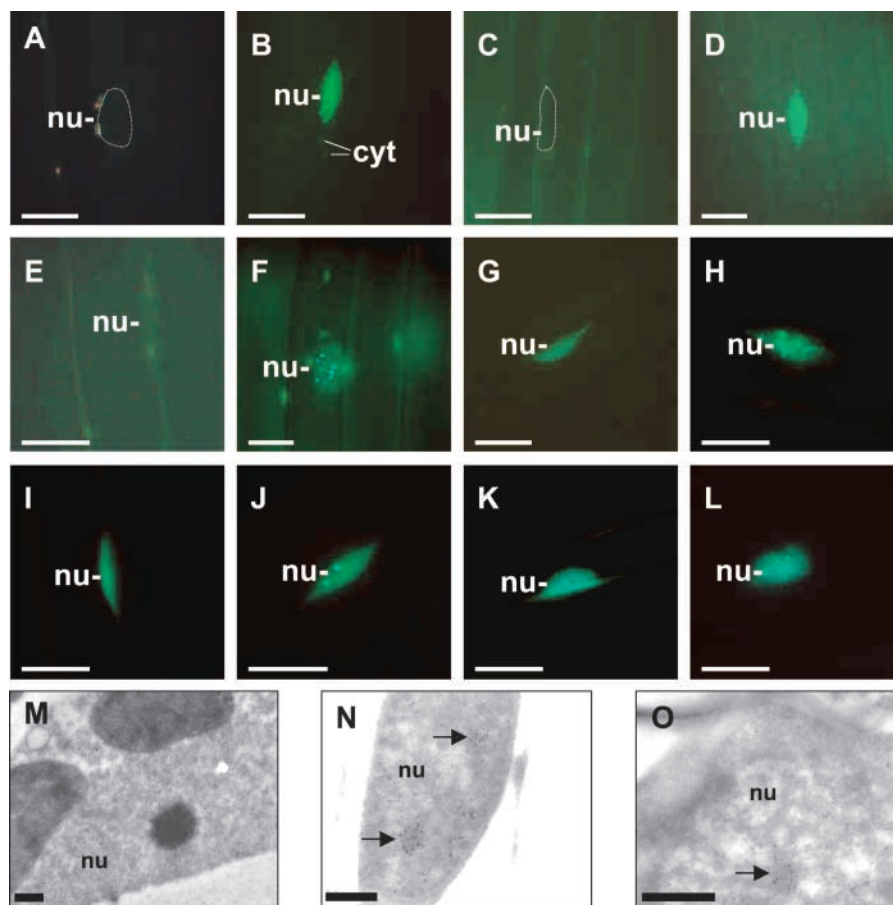


**Figure 2.** Nucleocytoplasmic Distribution and Formation of phyA to phyE:GFP-Containing Speckles in 7-Day-Old Dark-Adapted Seedlings Whose Germination Was Induced by 18 h of WL.

(A) to (L) Epifluorescence images of hypocotyl cells of transgenic *Arabidopsis* seedlings expressing the phyA:GFP (A) to (D), phyB:GFP (E) and (F), phyC:GFP (G) and (H), phyD:GFP (I) and (J), and phyE:GFP (K) and (L) fusion proteins. Epifluorescence images of nuclei of dark-adapted seedlings (A), (C), (E), (G), (I), and (K) and of seedlings transferred to WL for 10 min (B) or 6 h (F), (H), (J), and (L) or to FR for 6 h (D) are shown. Positions of selected nuclei (nu) are outlined (A) and (C), and speckled areas of cytosol (cyt) are indicated.

(M) to (O) Electron microscopic images of the cellular distribution and formation of intranuclear structures containing phyB. Seeds from transgenic *Arabidopsis* (line AB0 13) overexpressing phyB were germinated and grown in darkness. Electron microscopic images of nuclei of cotyledon cells from dark-adapted seedlings (M) and from seedlings transferred to R for 4 h (N) and (O) are shown. Arrows indicate the positions of nuclear areas highly enriched for phyB. Bars represent 10  $\mu\text{m}$  in (A) to (L) and 0.5  $\mu\text{m}$  in (M) to (O).

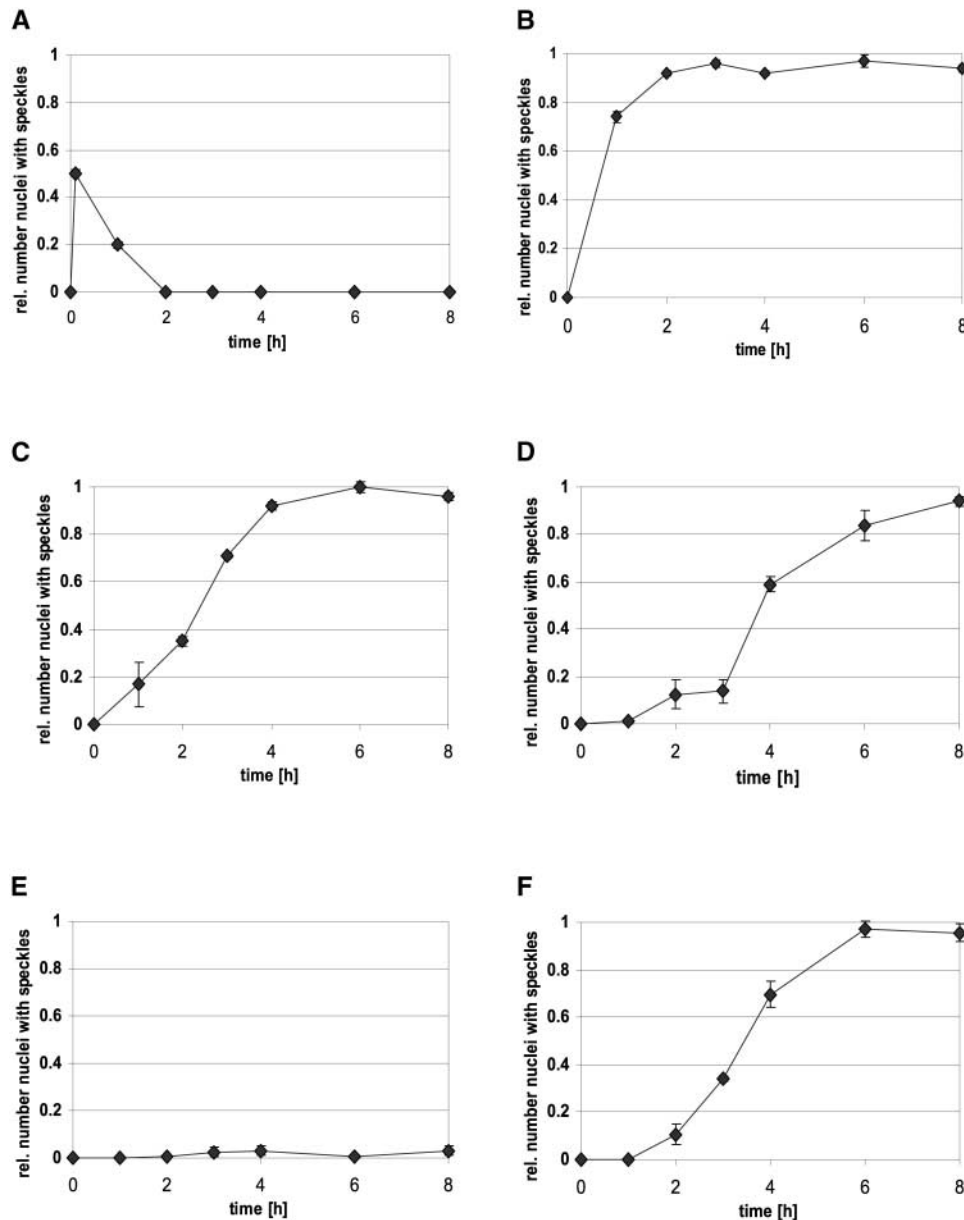


**Figure 3.** Kinetics of the Formation of Nuclear Speckles in Transgenic Arabidopsis Seedlings Expressing phyA to phyE:GFP Fusion Proteins.

Seven-day-old dark-adapted seedlings were irradiated for 8 h with FR (**B**) or WL (**A**) and (**C**) to (**F**), and nuclei of hypocotyl cells were analyzed by epifluorescence microscopy at the times shown. The values reflect the relative numbers of nuclei containing phyA:GFP (**A**) and (**B**), phyB:GFP (**C**), phyC:GFP (**D**), phyD:GFP (**E**), and phyE:GFP (**F**) intranuclear speckles. For each time point, at least three independent experiments were performed. In a single experiment, ~80 nuclei were analyzed in five different seedlings.

phyA:GFP, a weak, diffuse stain was detected in the nuclei of a number of cells (data not shown). Although the number of these cells varied from experiment to experiment, this observation indicates that the translocation of phyB:GFP into the nuclei can occur in these dark-adapted seedlings in the absence of additional light treatment.

Irrespective of the weak, diffuse nuclear staining, irradiation of these dark-adapted seedlings with WL strongly changed the subcellular distribution of phyB:GFP, similar to phyA:GFP, by promoting the import of the fusion protein into the nuclei. Translocation of phyB:GFP to the nucleus, however, was 1 order of magnitude slower and reached its

maximum level after 6 h (Figures 2F and 3C). PhyB:GFP localized in the nucleus, like phyA:GFP, formed characteristic speckles.

Analysis of the subcellular distribution of native phyB by electron microscopy in 7-day-old transgenic seedlings overexpressing phyB corroborated these findings. Immunogold labeling using a specific monoclonal anti-phyB antibody indicated that the nuclei of dark-adapted seedlings did not contain significant amounts of phyB (Figure 2M), whereas 4 h of R treatment induced a significant amount of phyB in the nuclei (Figures 2N and 2O). More importantly, the distribution of gold particles within the nucleus closely resembled the distribution of GFP-fluorescing speckles (Figures 2F, 2N, and 2O).

Interestingly, nuclear accumulation of the phyC:GFP, phyD:GFP, and phyE:GFP fusion proteins was readily detectable in 7-day-old dark-adapted transgenic seedlings whose germination was induced by an 18-h WL treatment at day 2. In these seedlings, phyC:GFP, phyD:GFP, and phyE:GFP accumulated in the nuclei displayed intense, diffuse staining (Figures 2G, 2I, and 2K, respectively), but no speckles were formed. WL irradiation induced the formation of phyC:GFP- and phyE:GFP-containing speckles in all nuclei monitored.

The kinetics of the appearance of the phyC:GFP- and phyE:GFP-containing speckles was comparable to that of phyB:GFP. In the case of phyC:GFP and phyE:GFP, the first fluorescent, nucleus-localized speckles were detectable after 2 h of light treatment, and their accumulation reached the saturation level after 6 h (Figures 2H, 2L, 3D, and 3F, respectively). In contrast, although WL induced the formation of phyD:GFP-containing speckles within the nuclei (Figure 2J), this process did not display an obvious maximum, and the number of nuclei containing fluorescent speckles remained low and variable during the 8-h period (Figure 3E).

To determine whether the diffuse GFP staining detected in the nuclei of 7-day-old dark-adapted seedlings was induced by the 18-h WL irradiation applied at day 2, we performed the following experiments. Seeds were allowed to imbibe at 4°C in water, and germination was induced by gibberellic acid (GA) in the dark. After imbibition, the emerging seedlings were grown for an additional 5 days at 25°C, also in darkness. Alternatively, after the cold treatment, seeds were irradiated hourly with 5-min pulses of R, R/red glass no. 9 (RG9), or RG9 for 18 h and then grown for 4 days at 25°C in darkness. Subcellular distribution of the phy:GFP fusion proteins was monitored at day 7 as described above.

We found that irrespective of growth conditions, phyA:GFP was localized exclusively in the cytosol. By contrast, in GA-treated phyB to phyE:GFP-expressing transgenic seedlings, GFP fluorescence was detectable only as diffuse staining of nuclei. Figure 4 shows that the import of phyB to phyE:GFP into the nuclei took place under all conditions, albeit at different levels. In seedlings that were never exposed to light during germination, diffuse staining of nuclei was detected in 8, 11, 14, and 25% of cells expressing

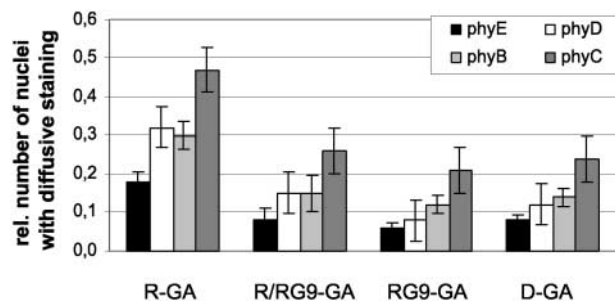


**Figure 4.** Nucleocytoplasmic Distribution of phyB to phyE:GFP in 7-Day-Old Dark-Adapted Seedlings Whose Germination Was Induced by GA.

D-GA seeds were germinated in complete darkness in the presence of GA. The hormone treatment was supplemented with 5-min hourly R pulses (R-GA) or R/RG9 pulses (R/RG9-GA) or RG9 pulses (RG9-GA) for 18 h after the cold treatment at day 2. Numbers indicate the relative number of nuclei showing GFP fluorescence (nuclei with GFP fluorescence/total number of nuclei monitored). For each experiment, 70 hypocotyl cells were monitored. phyB, phyC, phyD, and phyE are represented by light-gray, dark-gray, white, and black bars, respectively.

phyE:GFP, phyD:GFP, phyB:GFP, and phyC:GFP, respectively.

Figure 4 also shows that 18 hourly applied R pulses (equivalent to the 18-h WL treatment at day 2) followed by 4 days of growth in darkness significantly increased the percentage of nuclei exhibiting diffuse staining (20, 30, 32, and 48% for phyE, phyB, phyD, and phyC, respectively). RG9 pulses given immediately after R pulses erased the inductive effect of R, whereas RG9 pulses alone were not inductive (Figure 4). Note that the percentage of cells exhibiting diffuse nuclear staining did not differ significantly in seedlings grown in darkness or in seedlings that were treated subsequently with hourly R/RG9 or RG9 pulses, applied at day 2, after the cold treatment.

#### Mutant phyA:GFP and phyB:GFP Photoreceptor Molecules, Inactive Physiologically and Defective in Signaling, Are Imported into the Nuclei but Do Not Form Speckles

Wagner and Quail (1995) reported the isolation of a series of mutant phyA and phyB alleles whose overexpression did not change significantly the phenotypes of transgenic Arabidopsis plants. Detailed analysis of these mutant photoreceptor molecules revealed that (1) all of these mutants were created by amino acid substitutions, and (2) the mutations were localized invariably in a specific domain within the C-terminal region of phyA and phyB. Recently, Ni et al. (1999) reported that the ability of these mutant phyA and phyB molecules to interact with PIF3 *in vitro* was compromised

severely or eliminated. PIF3 has been shown to be an integral component of phyA- and phyB-regulated light-induced signaling (Martinez-Garcia et al., 2000). Therefore, the observations by Ni et al. (1999) suggest that these mutations interrupt the phyA- and phyB-controlled signaling cascades.

To characterize these mutants at the molecular level and in a more detailed manner in planta, we expressed one phyA and two phyB mutants fused to GFP in transgenic plants and compared their subcellular distribution to that of wild-

type phyA:GFP and phyB:GFP. Figure 5 (top) shows the positions and nature of the amino acid changes in these mutant phytochrome molecules and depicts the structures of the transgenes whose expression in planta was driven again by the viral 35S promoter. Figure 5 also shows that in 7-day-old dark-adapted seedlings (germination was induced by 18 h of WL), subcellular distribution of the mutant phy:GFP fusion proteins was nearly indistinguishable from that of wild-type phyA:GFP and phyB:GFP. That is, both the wild-type (Figure

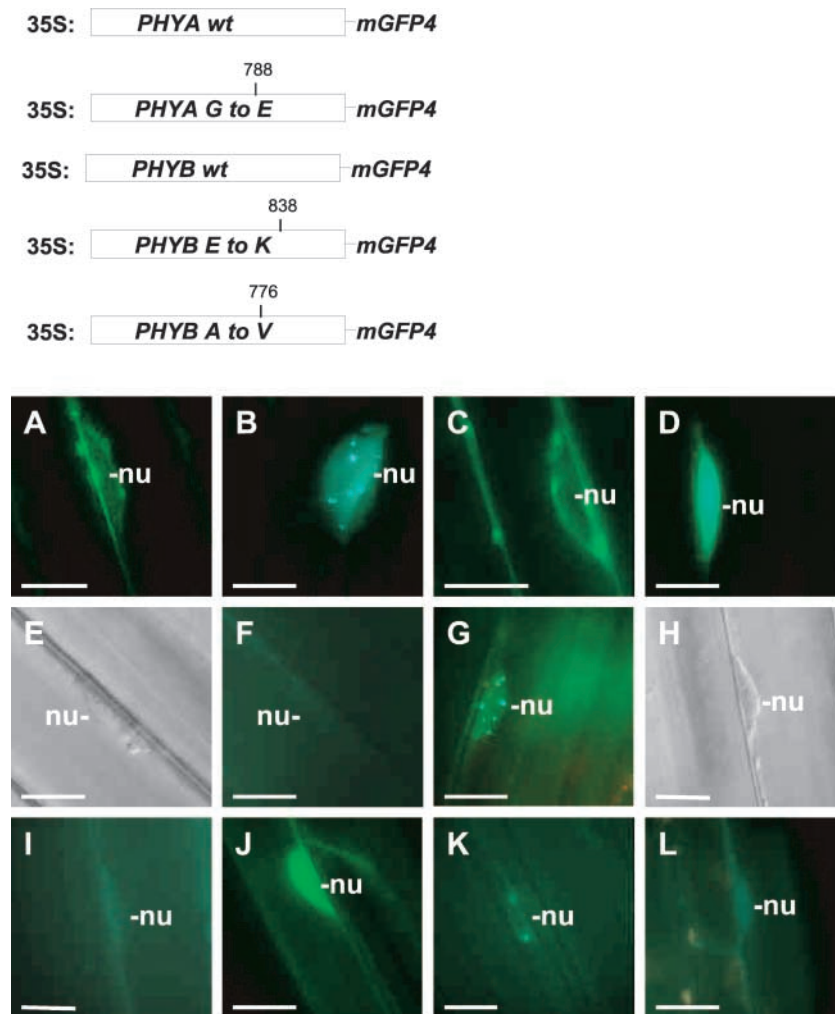


**Figure 5.** The Formation of Intracellular Speckles Is Not Detectable in Transgenic Plants Expressing Mutant phyA:GFP or phyB:GFP Fusion Proteins.

The top shows a diagram of the wild-type (wt) and mutant PHYA:GFP and PHYB:GFP transgenes expressed in Arabidopsis plants. Expression of these transgenes was driven by the viral 35S promoter. The positions of the amino acid substitutions within the mutant phyA and phyB molecules are shown. (A) to (L) show epifluorescence images ([A] to [D], [F], [G], and [I] to [L]) or differential interference contrast images ([E] and [H]) of nuclei in hypocotyl cells in 7-day-old seedlings expressing wild-type phyA:GFP ([A] and [B]) and phyB:GFP ([E] to [G]) and the mutant phyA:GFP ([C] and [D]) and phyB:GFP fusion proteins (position 838 ([H] to [J]) and position 776 ([K] and [L])) either at the end of dark incubation ([A], [C], [E], [F], [H], [I], and [K]) or after 9 h of FR ([B] and [D]) or 18 h of R ([G], [J], and [L]). (E) and (F) and (H) and (I) are pairs that represent the same cells. Positions of the selected nuclei are indicated (nu). Bars = 10  $\mu$ m.

5A) and mutant (Figure 5C) phyA:GFP fusions were localized exclusively in the cytosol, and no nuclear GFP fluorescence was detectable.

Similar results were obtained by analyzing the subcellular distribution of the wild-type and mutant phyB:GFP molecules (Figures 5E, 5F, 5H, 5I, and 5K). However, in ~25% of cells expressing the wild-type phyB:GFP or the mutant phyB:GFP molecules, a weak, diffuse nuclear fluorescence was detectable (data not shown). Light treatment of dark-grown seedlings expressing wild-type phyA:GFP or phyB:GFP induced nuclear import and accumulation and the appearance of speckles (Figure 5B and 5G, respectively). Irradiation of dark-grown seedlings expressing the mutant phyA:GFP and phyB:GFP fusion proteins also induced nuclear import of the tagged photoreceptor derivatives. However, accumulation of the mutant phyA:GFP and phyB:GFP fusion proteins in the nuclei, in sharp contrast to that of the wild-type phy:GFPs, was not accompanied by the formation of speckles (Figures 5D, 5J, and 5L, respectively).

Moreover, we found that, independent of the duration of irradiation, nuclear staining remained diffuse, and we were able to detect only the sporadic appearance of one or two speckles (data not shown). These observations suggest that the mutant phyA and phyB molecules that do not interact with PIF3 *in vitro* and that are inactive physiologically in planta still are imported into the nuclei in a light-induced manner but lose their capacity to induce the formation of speckles that are characteristic of the wild-type phyA:GFP and phyB:GFP fusion proteins.

### The Appearance of phy:GFP Speckles in the Nuclei Is Regulated by Diurnal Oscillation

We also analyzed the kinetic features of the intracellular distribution of phyA to phyE:GFP fusion proteins in transgenic seedlings grown under natural light/dark conditions. To this end, seedlings were germinated in darkness, transferred to a phytochamber at day 7, and grown for an additional 48 h under 8-h-WL/16-h-dark diurnal cycles. In the case of phyA:GFP, transgenic seedlings were grown under 8-h-FR/16-h-dark diurnal cycles. The intracellular distribution of the phyA to phyE:GFP fusion proteins was monitored during a 48-h period representing two consecutive diurnal cycles. In these experiments, as described above, we detected two types of GFP fluorescence. Nuclear staining, in the case of phyB:GFP-expressing seedlings, was attributable mainly to periodically appearing intranuclear speckles in the background of a constant, very weak, diffuse fluorescence.

By contrast, in the nuclei of phyC to phyE:GFP-expressing seedlings, diffuse but relatively intense fluorescence with periodically appearing intranuclear speckles was detected. The diffuse nuclear fluorescence, independent of its intensity, did not fluctuate significantly during the light/dark cycles. Therefore, the data plotted in Figure 6B show the absolute number of intranuclear phyB:GFP speckles, whereas

Figures 6A, 6C, 6D, and 6E indicate the percentage of cells in which intranuclear phyA:GFP and phyC to phyE:GFP speckles, respectively, were detectable. Note that the heterogeneous, patchy expression pattern and the low number of speckles detectable in phyD:GFP-expressing seedlings prevented us from obtaining statistically reliable data (Figure 6D).

However, based on the criteria described above, it is evident that the speckle formation associated with the phyB:GFP fusion protein displayed a diurnal oscillation. Figure 6B shows that the number of nuclear speckles containing phyB:GFP was low in nuclei 2 h before the light-on signal. The absolute number of intranuclear speckles containing phyB:GFP (Figure 6B) increased dramatically 10 min before the light-on signal (still in darkness) and increased until the end of the light period. Intranuclear speckle formations in phyA and phyC to phyE:GFP-expressing seedlings followed similar kinetics. Figure 6 shows that the number of cells in which intranuclear phyA:GFP-associated (Figure 6A), phyC:GFP-associated (Figure 6C), and phyE:GFP-associated (Figure 6E) speckles were detectable increased again significantly 10 min before the light-on signal compared with levels detected at the middle of the dark period. These levels increased further during the light phase, and the maximum values were detected, uniformly for all phy:GFP species except phyD:GFP, at the end of the light period before the light-off signal.

Figure 7 shows representative photographs taken to determine (1) the number of speckles containing phyB:GFP (Figures 7A to 7C) and (2) the number of cells containing phyE:GFP intranuclear speckles (Figures 7G to 7I) at selected time points during the experiments. More importantly, as Figures 7D to 7F illustrate, electron microscopic analysis of the distribution of phyB in AB0 lines indicates that the appearance of subnuclear structures, enriched highly for phyB protein, also followed a characteristic diurnal rhythm.

In addition, our observations indicate that after the light-off signal, the number of nuclei displaying intranuclear speckles (phyA, phyC, and phyE:GFP) and the absolute number of intranuclear speckles (phyB:GFP) within the nuclei decreased rapidly. The depletion was fastest for phyB and phyC:GFP and slowest for phyA:GFP. The increase in the number of intranuclear speckles (phyB:GFP) and in the number of nuclei containing phyA and phyC to phyE:GFP-associated speckles around the dark/light transition could indicate that (1) the nuclear import or (2) the apparent compartmentalization of phy:GFP fusion proteins within the nuclei is regulated differentially in seedlings grown in light/dark cycles and in etiolated material at the time of the first light treatment.

## DISCUSSION

Different members of the phytochrome family represent an ideal group of photoreceptors for monitoring subtle changes in the light environment. The molecular and photobiological



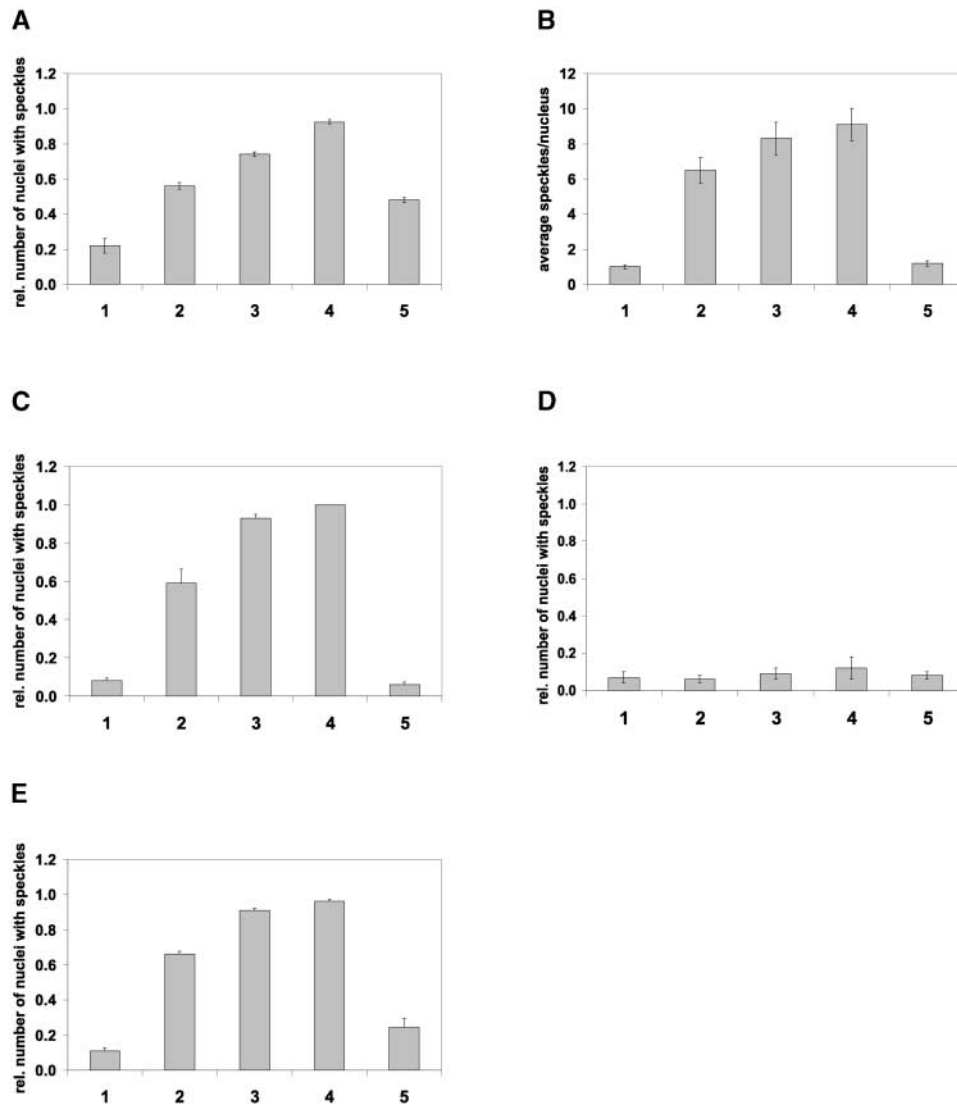


**Figure 6.** The Appearance of phyA to phyE:GFP Speckles in the Nuclei Exhibits a Diurnal Rhythm in Transgenic Arabidopsis Plants Grown under Short-Day Conditions.

Quantitative analysis of the formation of speckles in the nuclei of hypocotyl cells of phyA:GFP-expressing (A), phyB:GFP-expressing (B), phyC:GFP-expressing (C), phyD:GFP-expressing (D), and phyE:GFP-expressing (E) transgenic Arabidopsis seedlings. Seedlings were germinated and grown in darkness and transferred subsequently to short-day conditions (8 h of WL/16 h of darkness [(B) to (E)] or 8 h of FR/16 h of darkness [A]) for 48 h. The absolute number of nuclear speckles (B) or the relative number of nuclei containing speckles [(A) and (C) to (E)] were determined at 2 h before (bar 1), 10 min before (bar 2), 1 h after (bar 3), and 4 h after (bar 4) the onset of the third light period or 8 h after the onset of the third dark period (bar 5). For each time point, at least 80 nuclei (20 nuclei in four or five independent seedlings representing one type of transgenic material) were analyzed in three consecutive experiments.

studies described here demonstrate that (1) all five phytochrome species are imported into the nuclei, and (2) translocation of individual phytochromes into the nuclei is regulated differentially by light.

Expression and analysis of tagged phyB (Sakamoto and Nagatani, 1996) and phyA (Kircher et al., 1999) fusion pro-

teins resulted in the first information regarding the light-regulated nucleocytoplasmic distribution of phytochromes in transgenic plants. These and subsequent studies showed that the phyA and phyB:GFP fusion proteins represent functional photoreceptors (Yamaguchi et al., 1999; Gil et al., 2000; Kim et al., 2000). It also was established that import of

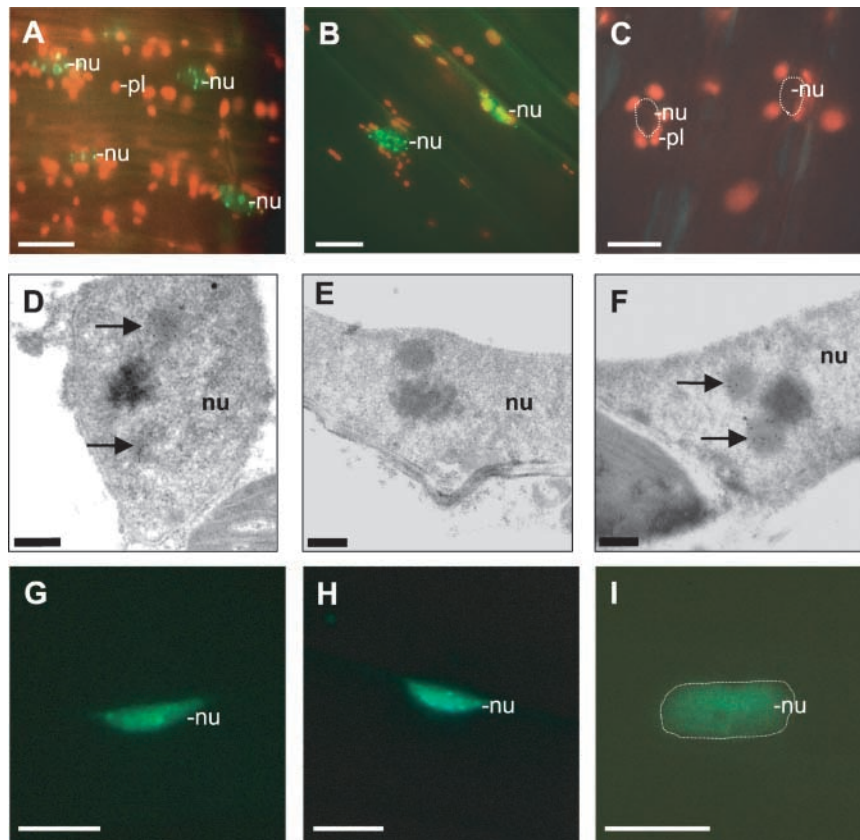


**Figure 7.** Epifluorescence and Electron Microscopic Images of Nuclei of Hypocotyl Cells from Seedlings Expressing the phyE:GFP and phyB:GFP Fusion Proteins during a Diurnal Cycle.

Epifluorescence microscopy images illustrate the accumulation of phyB:GFP in the nuclei 4 h after the onset of light (middle of day) (**A**) or 4 h (**B**) and 8 h (**C**) after the onset of the dark period. Electron microscopic images illustrate the formation of intranuclear structures enriched highly for phyB 4 h after the onset of the light period (**D**), 8 h after the onset of the dark period (**E**), and in the middle of the subsequent light period (**F**). Epifluorescence images represent the accumulation of phyE:GFP speckles in the nuclei 10 min before (**G**) or 1 h after (**H**) the start of the second light period or 4 h after the onset of the third dark period (**I**). Positions of nuclei (nu) are outlined (**C**) and (**I**). Positions of selected plastids (pl) also are indicated. Intranuclear structures are marked by arrows. Bars represent 10  $\mu\text{m}$  in (**A**) to (**C**) and (**G**) to (**I**) and 0.5  $\mu\text{m}$  in (**D**) to (**F**).

phyA and phyB photoreceptors into the nuclei is a light-dependent process and that phyA and phyB localized in the nuclei form characteristic speckles (Kircher et al., 1999; Yamaguchi et al., 1999), similar to those observed for COP1:GFP (Ang et al., 1998). Furthermore, the pattern of subcellular distribution and the kinetics of speckle formation for the phyA and phyB:GFP fusion proteins remained unchanged and were completely independent of the level of overexpression (Kircher et al., 1999; Kim et al., 2000).

#### Import of phyA to phyE into the Nuclei Is Regulated Differentially by Light

In this article, we demonstrate that all five phytochrome species are imported into the nuclei (Figures 2 to 4) and that this

process is regulated differentially by light. In dark-adapted seedlings that exhibit the characteristic etiolated phenotype, phyA:GFP is localized exclusively in the cytosol. Import of phyA:GFP into the nuclei is strictly light induced, is accompanied by immediate speckle formation, and is a rapid process. PhyB is thought to be the major photoreceptor for light-grown plants. We show that in the majority of cells in dark-grown seedlings, regardless of the germination protocol applied, phyB:GFP is not detectable in the nuclei.

R or WL uniformly induced the import of phyB into the nucleus, which is accompanied, as in phyA:GFP, by speckle formation. However, in contrast to phyA:GFP, phyB:GFP is not localized exclusively in the cytosol of dark-adapted seedlings. In  $\sim 10\%$  of cells, even in seedlings that were germinated in darkness in the presence of GA, a weak, diffuse staining of nuclei was detectable. Notwithstanding this sporadically occurring,

diffuse staining, WL and R treatment increased the amount of phyB:GFP localized in the nuclei significantly and promoted speckle formation, reaching saturation within 6 to 8 h.

The subcellular distribution of phyC to phyE:GFP, depending on the germination protocol used, differed sharply from that of phyA and phyB. When germination was induced by 18 h of WL after cold treatment at day 2, nuclei of 7-day-old dark-adapted seedlings expressing the phyC to phyE:GFP fusion proteins showed intense diffuse staining. Additional WL or R treatment induced the formation of speckles in the nuclei without significantly affecting the intensity of diffuse staining. However, when transgenic seeds were germinated in complete darkness in the presence of GA, the import of phyC to phyE:GFP, like that of phyB:GFP, occurred at very low levels and was detectable in only ~10% of the cells. Additional WL or R treatment of these seedlings promoted speckle formation. Note that regardless of whether the nuclei showed diffuse staining, the kinetics of speckle formation did not differ significantly after the second WL or R treatment.

To explain these findings, we propose the following models. In seedlings that were grown in the presence of GA or were irradiated with only RG9 pulses, the import of phyB to phyE:GFP occurred before germination (presumably in their Pfr form) or a very low level import of Pr conformers occurred during germination and seedling development. Kircher et al. (1999) showed that the Pr form of tobacco phyB:GFP is localized exclusively in the cytosol; therefore, we favor the first explanation. Furthermore, we note that because of the RG9 treatment, >99.9% of phytochrome molecules are in their Pr form. Thus, the diffuse staining detected in these seedlings, independent of the timing of the translocation or conformation of the imported proteins, likely represents Pr forms of these phytochrome species.

In seedlings whose germination was induced by 18 h of WL or R treatments, the first light treatment generated Pfr forms of phyA to phyE:GFP and promoted the subsequent import of these fusion proteins into the nuclei. Indeed, we show that hourly applied short R pulses, equivalent of the 18-h WL treatment at day 2 after imbibition, significantly increased the number of nuclei exhibiting diffuse staining at day 7 compared with that of the GA control. More importantly, RG9 pulses reversed the inductive effect of R, whereas RG9 pulses alone were completely ineffective at enhancing the nuclear import of phyB to phyE:GFP fusion proteins. These observations are in good agreement with our previous finding (Kircher et al., 1999) and strongly suggest that all phytochromes are imported into the nuclei in their Pfr forms.

### The Light-Induced Formation of phyA to phyE:GFP-Containing Speckles in the Nuclei Is a Characteristic Feature of Physiologically Active Photoreceptors

The appearance of speckles is triggered exclusively by light, and the kinetics of speckle formation is different between members of the phytochrome family. Notably, the import of

phyA:GFP is always accompanied by immediate speckle formation that occurs within minutes. The accumulation of phyB:GFP-containing speckles in the nuclei is 1 order of magnitude slower. The kinetics of speckle formation of phyC and phyE:GFP is similar to that of phyB:GFP, whereas that of phyD:GFP is by far the slowest. This latter finding is fairly surprising because sequence analysis demonstrated that the *PHYD* gene probably is a recent duplication of *PHYB*. The data presented here, however, clearly demonstrate marked differences in the nucleocytoplasmic distribution of phyB and phyD. We speculate that the differential responsiveness of these photoreceptors to excitation might be manifested at the level of speckle formation.

In this context, WL and R are similarly effective at inducing the formation of phyB- to phyE-containing speckles, indicating that these photoreceptors are operative in R. The only exception to this is phyA, which accumulates only transiently in the nuclei in WL (Figure 2B) and R (Kim et al., 2000). Furthermore, phyA:GFP is the only phytochrome that shows fast cytosolic speckle formation before nuclear translocation (Kircher et al., 1999; Kim et al., 2000). The rapid loss of nuclear staining and the cytosolic speckle formation in R and WL can be interpreted as biological reflections of the fact that phyA is the only phytochrome that shows fast degradation in its Pfr form.

If speckle formation is a feature of functional phytochrome, what is the biological significance of the observed diffuse staining by phyB to phyE:GFP in the nuclei of etiolated seedlings? The germination of *Arabidopsis* requires light and is regulated by phyA, phyB, phyD, and phyE (Poppe and Schäfer, 1997). Five days after the induction of germination with WL, we detected in 7-day-old etiolated seedlings expressing phyB to phyE:GFP diffuse staining of the nuclei, whereas phyA:GFP was localized exclusively in the cytosol.

These data indicate that the import of phyB to phyE:GFP into the nuclei had occurred, yet the seedlings still exhibited the etiolated phenotype. Thus, we propose that the diffuse staining of nuclei by phyB to phyE, like that observed for the mutant phyA and phyB molecules (see below) at this developmental stage, indicates the inactive signaling status of these photoreceptors, at least regarding deetiolation.

### Physiologically Inactive Mutant phyA and phyB Are Imported into the Nuclei in a Light-Dependent Manner but Do Not Form Speckles

We demonstrate that the nucleocytoplasmic distribution of mutant alleles of phyA and phyB, which were shown to be impaired in interacting with PIF3 *in vitro* (Ni et al., 1999) and inactive in mediating light-induced signaling *in vivo* (Wagner and Quail, 1995), is indistinguishable from that of wild-type phyA and phyB. These data suggest that these point mutations, which are localized in the C-terminal region of phyA and phyB, do not interfere with the light-dependent partitioning of the photoreceptors. This conclusion is further supported by the

fact that translocation of these molecules into the nucleus was regulated similarly by light under all conditions examined.

Note that the intensity of nuclear staining of the phyB 776 mutant was significantly weaker compared with that of other phyB:GFP fusion proteins in all transgenic plants analyzed. This observation indicates that this point mutation within the phyB molecule might affect, in addition to the interaction with PIF3, other properties of the photoreceptor, such as degradation and/or folding.

Moreover, we provide evidence that the light-regulated nuclear import of mutant phyA and phyB:GFP molecules is not associated with the formation of speckles in either dark- or light-grown material regardless of the duration of light treatment. On the one hand, these observations show a strong correlation between speckle formation and the biological activity of photoreceptors and underscore the importance and usefulness of these structures in monitoring phytochrome-mediated signaling. On the other hand, we suggest that the interaction of phyA, phyB, and possibly other phytochromes with their confirmed/putative signaling partners in the nuclei is required to detect light-induced speckle formation in the nuclei.

### The Appearance of phyA to phyE:GFP-Associated Speckles in the Nuclei Exhibits a Diurnal Rhythm

The different phytochromes have specialized roles to regulate plant growth and development during seasonal changes in the light environment (Devlin et al., 1998, 1999). Here, we report that the amount of nucleus-localized phyB and the number of cells containing phyA, phyC, and phyE:GFP fusion proteins as speckles exhibit a diurnal oscillation in plants grown in 8-h-light/16-h-dark cycles. According to our interpretation, these observations could indicate that the nucleocytoplasmic distribution and/or biological activity of phyA to phyE localized in the nuclei is modulated by a diurnal oscillation and that this is mediated, at least partly, at the level of nuclear import.

Note that diurnal oscillation in the number of cells containing phyA:GFP in the nucleus can be detected only under 8-h-FR/16-h-dark cycles and not under 8-h-WL/16-h-dark cycles. Under these conditions, the amount of Pfr formed by FR probably is not sufficient to induce the nuclear translocation or formation of speckles of any other phytochrome (for wavelength dependence of the nuclear import of phyB, see Gil et al., 2000). Thus, these results indicate that phyA is the major photoreceptor that is capable of responding to R/FR in intense shade. We also demonstrate that the kinetics of the changes in the amount of phyB:GFP localized in the nuclei and the number of cells containing nucleus-localized phyC to phyE:GFP speckles (elicited by light/dark and dark/light transitions in plants grown under diurnal conditions) are faster/greater than the same values observed in etiolated seedlings during the first light treatments.

As for phyB, phyC, and phyE:GFP, the velocity of nuclear import after diurnal entrainment increased twofold to threefold; for phyD:GFP, the increase was not significant. How-

ever, the molecular mechanism by which preirradiations strongly enhance the sensitivity of speckle formation is not understood at present. Regardless of the mechanism responsible for mediating this phenomenon, these findings are surprising and of general interest for the following reason: phyA to phyE were shown to be bona fide input receptors for the plant circadian system (Somers et al., 1998).

Here, we show that the appearance of speckles in the nuclei increased well before the light-on signal. The anticipation of the subjective light period at the level of import and accumulation of speckles suggests regulation by the circadian clock. This theory is especially exciting because phyB Pfr has been shown to interact with PIF3 bound to the CCA1 promoter (Martinez-Garcia et al., 2000). However, demonstration of the involvement of the circadian clock in the regulation of phyB compartmentalization requires additional experiments performed under free-running conditions. Note that the number of phyB:GFP-containing nuclear speckles decreased rapidly in light/dark-grown seedlings after the end of the light period (Figure 7B).

PhyB is believed to inhibit hypocotyl growth in subsequent darkness (Elich and Chory, 1997); thus, our observation can be interpreted as indicating that speckle formation is not required to mediate this phyB-regulated response. However, the inhibition of hypocotyl growth is a complex phenomenon, it is mediated by different signaling pathways, and it is not understood at the molecular level. Accordingly, phyB speckles in subsequent darkness could rapidly activate a yet unknown signaling cascade. Thus, our results do not necessarily contradict the proposed biological significance of speckles in phyB-mediated signaling.

Moreover, our electron microscopic studies indicate that phyB imported into the nuclei is not distributed randomly. Immunogold-labeled phyB is detectable mainly in dense, defined areas of nuclei whose number and appearance after light treatments or during light/dark cycles show obvious similarities to those of phyB:GFP-containing speckles. Although the molecular function of these subnucleus-like bodies or phyB-containing speckles is not yet defined, it is tempting to propose that these structures represent phyB-containing protein complexes. However, it remains to be determined whether the oscillating transcription of CCA-1 or of other unidentified genes required for a functional circadian network in plants (Wang and Tobin, 1998) is regulated, at least partly, via the oscillating levels of Pfr phyB localized in these subnucleus-like structures.

## METHODS

### Light Sources

Handling of irradiated and dark-grown seedlings under a dim-green safelight and the white, red, and far-red light sources used in these studies have been described previously (Kircher et al., 1999).

### Plant Material and Growth Conditions

Transgenic *Arabidopsis thaliana* lines were generated in a Wassilewskija ecotype lacking functional phytochrome D (phyD) photoreceptor as described in Aukerman et al. (1997). Transgenic *Arabidopsis* seeds were germinated by two markedly different experimental protocols. In one case, seeds were sown on four-layer sterile filter paper and allowed to imbibe in sterile water in the dark for 48 h at 4°C. Cold-treated seeds then were irradiated with 18 h of white light to induce homogeneous germination, transferred to 25°C, and grown for 4 additional days in the dark.

In the other case, seeds were sown on four-layer sterile filter paper and allowed to imbibe in sterile water supplemented with gibberellic acid (GA) (1:1000 dilution in a stock solution of 346.4 mg/mL; Sigma) in the dark for 48 h at 4°C. Cold-treated GA-induced seeds then were transferred to 25°C and grown for an additional 5 days. Alternatively, after the cold treatment, GA-induced seeds were irradiated hourly with 5 min of red light or red light followed by RG9 or RG9 pulses for 18 h and then transferred to 25°C and grown for an additional 4 days.

Dark-grown seedlings were manipulated under dim-green safelight. Seven-day-old dark-grown seedlings obtained as described above were subjected to various light treatments as described in Results. Modified Leitz Prado 500-W universal projectors (Leitz, Wetzlar, Germany) were used as light sources for pulse irradiation with Osram Xenophot Longlife lamps (Osram, München, Germany). Red light was obtained by passing the light beam through a Balzers KG65 filter (Balzers, Vaduz, Liechtenstein) with maximal transmission at 650 nm (bandwidth of 15 nm), whereas far-red light was obtained using an 8-mm-thick RG9 cutoff filter (Schott, Mainz, Germany) with maximal transmission at 775 nm. Light intensity in both cases was 10  $\mu\text{mol}\cdot\text{m}^{-2}\cdot\text{s}^{-1}$ . Hypocotyl measurements were performed manually, and SE values of the mean did not exceed 12%.

### Recombinant DNA Technology and Construction of the PHY:Green Fluorescent Protein Chimeric Genes

Construction of the 35S:PHYA:green fluorescent protein (GFP) chimeric gene has been described in Kim et al. (2000). To facilitate the construction of the 35S:PHYB to PHYE:GFP fusion genes, the 5' and 3' regions of the full-length *PHYB* to *PHYE* cDNA clones as well as those of the modified GFP4 (mGFP4) gene were modified by PCR as follows. mGFP4 was modified by introducing a unique Ehel site in front of the ATG and a unique SacI site after the stop codon. The product was transferred into the modified pPCV812 binary vector originally described in Koncz et al. (1994). The modified pPCV812 binary vector contained unique BamHI, XbaI, Sall, and SmaI sites between the 35S promoter and the nopaline synthase (NOS) transcription terminator region.

mGFP4 was transferred into the pPCV812 as a SmaI-SacI fragment between the 35S promoter and the NOS 3' transcription terminator. The *PHYB* cDNA was modified by the introduction of a unique XbaI site in front of its ATG, and its stop codon was replaced by the insertion of a unique StuI site. The *PHYC*, *PHYD*, and *PHYE* cDNAs were modified by the insertion of unique SmaI and BamHI sites, in front of their ATGs, and their stop codons were replaced by inserting unique Ehel sites.

PCR products were purified, digested with restriction enzymes, and cloned directly into the linker region of the modified pPCV812 vector containing the 35S promoter:mGFP4:NOS cassette. Before transfer into *Agrobacterium tumefaciens*, selected clones were

sequenced partially across the junction regions of the PHY:mGFP4 fusions. All DNA manipulations were performed as described in Sambrook et al. (1989), and PCR was performed using the Proof-Sprinter polymerase system (AGS, Heidelberg, Germany).

### Plant Transformation and Regeneration of Transgenic Arabidopsis Lines

The pPCV812 binary vectors containing the 35S:PHYA to PHYE:GFP:NOS chimeric genes were transferred from *Escherichia coli* to *Agrobacterium* GV3101. *Arabidopsis* plants were transformed via the infiltration method. Transgenic plants were selected on sterile medium containing hygromycin (15  $\mu\text{g}/\text{mL}$ ) and transferred to the greenhouse after 2 weeks. Selected plants were grown to maturation. Selfed and homozygous segregants were identified. Homozygous lines selected were multiplied, and the seeds obtained were used in all experiments described. For each construct, we generated at least 15 independent lines.

### Epifluorescence, Light, and Confocal Microscopy

For epifluorescence and light microscopy, seedlings were transferred to glass slides and analyzed with an Axioskop microscope (Zeiss, Oberkochen, Germany). Excitation of phy:GFP was performed with standard isothiocyanate and GFP filter sets. For every time point and irradiation program, the number of speckles (seedlings expressing phyB:GFP) or the number of nuclei containing speckles (phyA, phyC, phyD, and phyE:GFP) were counted in 20 nuclei or cells, respectively. Each experiment was repeated three times using five independent seedlings. Mean values are shown, and SE values did not exceed 20%, with the exception of phyD:GFP-expressing seedlings.

Representative cells were documented by photography with an automatic Contax 167 MT camera (Kyocera, Tokyo, Japan) containing 64T film (Kodak AG, Stuttgart, Germany) scanned subsequently with an LS-1000 scanner (Nikon, Tokyo, Japan) or with a digital AxioCam camera system (Zeiss). Dark-grown plant material was manipulated under dim-green safelight before microscopy. Documentation of cells was performed during the first 5 min of microscopic analysis. Photographs were processed for optimal presentation using the Photoshop 5.0 (Adobe Systems Europe, Edinburgh, UK) and MS Office 97 (Microsoft, Redmond, WA) software packages.

### Protein Extraction, Protein Assays, SDS-PAGE, Protein Gel Blot Analysis, and Immunodetection

Two hundred milligrams of 7-day-old dark-grown *Arabidopsis* seedlings was homogenized in a potter using hot extraction buffer containing 65 mM Tris-HCl, pH 7.8, 4 M urea, 5% (w/v) SDS, 14 mM 2-mercaptoethanol, 15% (v/v) glycerol, and 0.05% (w/v) bromophenol blue. The homogenate was heated for 5 min at 95°C, the resulting suspension was cleared by centrifugation (10 min at 20,000g and 25°C), and the supernatant was used for further experiments. Protein assays were performed as described in Popov et al. (1975).

Twenty micrograms of crude protein extract was separated on an SDS-PAGE gel and blotted to a polyvinylidene difluoride membrane. Immunodetection of phyA to phyD was performed using the specific monoclonal antibodies (phyA-073D, phyB-B6-B3, phyC-C11, and phyD-2C1) described in Hirschfeld et al. (1998) as primary antibodies,

a peroxidase-coupled anti-mouse antiserum (Sigma-Aldrich) as a secondary antibody, and an alkaline phosphatase-coupled anti-goat antibody.

#### Immunogold Labeling and Electron Microscopy

Intact seedlings were fixed in cacodylate buffer containing 4% formaldehyde and 0.1% glutaraldehyde, dehydrated in alcohol, and embedded in Lowicryl resin (Serva, Heidelberg, Germany). Ribbons of ultrathin serial sections were collected on 200-mesh nickel grids. Immunolabeling was performed using PBS, pH 7.2, containing 1% BSA (Dianova, Hamburg, Germany) and 0.1% Tween 20 (Serva, Heidelberg, Germany). Before use, the saline solution was filtered through a 0.22- $\mu$ m filter (Millipore, Bedford, MA). The monoclonal antibody against phyB was diluted 1:100 in the same buffer. The second gold-coupled antibody was goat anti-rabbit antibody (particle size of 10 nm; Dianova) diluted 1:20 in the labeling buffer. Incubations of the grids on serum were performed for 60 min. In each experiment, several series of ultrathin sections from fixed material were labeled in parallel.

Electron microscopy was performed using a Philips CM10 electron microscope (Philips, Kassel, Germany) at 60 kV. Photographs were taken digitally using a Bioscan 972 camera (Gatan, München, Germany). Photographs were processed for optimal presentation using Photoshop 5.0 (Adobe) and MS Office 97 (Microsoft).

#### ACKNOWLEDGMENTS

We are grateful to Robert Sharrock for providing the full-length *Arabidopsis* *PHYB*, *PHYC*, *PHYD*, and *PHYE* cDNAs, to Peter Quail for providing the monoclonal anti-phyA to phyE antibodies, and to Rozsa Nagy and Erik Bury for expert technical assistance. Work in Germany was supported by grants from the Deutsche Forschungsgemeinschaft (SFB592), Landesforschungsschwerpunkt, the Human Frontier Science Programme, and Fonds der Chem. Industrie to E.S., a Humboldt research fellowship to T.H.-M., and the Wolfgang Paul Award to F.N. Work in Hungary was supported by grants from the Hungarian Science Foundation (T-032565), the Howard Hughes Medical Institute (HHMI International Scholarship), and the Human Frontier Science Programme to F.N. and a grant from the Deutsche Forschungsgemeinschaft to F.N. and E.S.

Received December 12, 2001; accepted April 3, 2002.

#### REFERENCES

- Ang, L.-H., Chattopadhyay, N.W., Oyama, T., Okada, K., Batschauer, A., and Deng, X.-W. (1998). Molecular interaction between COP1 and HY5 defines a regulatory switch for light control of *Arabidopsis* development. *Mol. Cell* **1**, 213–222.
- Aukerman, J.M., Hirschfeld, M., Wester, L., Weaver, M., Clack, T., Amasino, M.R., and Sharrock, A.R. (1997). A deletion in the *PHYD* gene of *Arabidopsis* Wassilewskija ecotype defines a role for phytochrome D in red/far-red light sensing. *Plant Cell* **9**, 1317–1326.
- Benfey, P.N., Ren, L., and Chua, N.-H. (1990). Combinatorial and synergistic properties of CaMV 35S enhancer subdomains. *EMBO J.* **9**, 1685–1696.
- Botto, J.F., Sanchez, R.A., and Casal, J.J. (1995). Role of phytochrome B in the induction of seed germination by light in *Arabidopsis thaliana*. *J. Plant Physiol.* **146**, 307–312.
- Clack, T., Matthews, S., and Sharrock, R.A. (1994). The phytochrome apoprotein family in *Arabidopsis* is encoded by five genes: The sequence and expression of *PHYD* and *PHYE*. *Plant Mol. Biol.* **25**, 413–417.
- Deng, X.W., Caspar, T., and Quail, P.H. (1991). Cop1: A regulatory locus involved in light-controlled development and gene expression in *Arabidopsis*. *Genes Dev.* **5**, 1172–1182.
- Devlin, P.F., Halliday, K.J., Harberd, N.P., and Whitelam, G.C. (1996). The rosette habit of *Arabidopsis thaliana* is dependent upon phytochrome action: Novel phytochromes control internode elongation and flowering time. *Plant J.* **10**, 1127–1134.
- Devlin, P.F., Patel, S., and Whitelam, G.C. (1998). Phytochrome E influences internode elongation and flowering time in *Arabidopsis*. *Plant Cell* **10**, 1479–1488.
- Devlin, P.F., Robson, P.R., Patel, S.R., Goosey, L., Sharrock, R.A., and Whitelam, G.C. (1999). Phytochrome D acts in the shade-avoidance syndrome in *Arabidopsis* by controlling elongation growth and flowering time. *Plant Physiol.* **119**, 909–915.
- Eichenberg, K., Baeurle, I., Paulo, N., Sharrock, R.A., Ruediger, W., and Schäfer, E. (2000). *Arabidopsis* phytochromes C and E have different spectral characteristics from those of phytochromes A and B. *FEBS Lett.* **470**, 107–112.
- Elich, T.D., and Chory, J. (1997). Biochemical characterization of *Arabidopsis* wild type and mutant phytochrome B holoproteins. *Plant Cell* **9**, 2271–2280.
- Furuya, M., and Schäfer, E. (1996). Photoperception and signalling of induction reactions by different phytochromes. *Trends Plant Sci.* **1**, 301–307.
- Gil, P., Kircher, S., Adam, E., Bury, E., Kozma-Bognar, L., Schäfer, E., and Nagy, F. (2000). Photocontrol of subcellular partitioning of phytochrome-B:GFP fusion protein in tobacco seedlings. *Plant J.* **22**, 135–145.
- Haseloff, J., Siemering, K.R., Prasher, D.C., and Hodge, S. (1997). Removal of a cryptic intron and subcellular localization of green fluorescent protein are required to mark transgenic *Arabidopsis* plants brightly. *Proc. Natl. Acad. Sci. USA* **94**, 2122–2127.
- Hirschfeld, M., Tepperman, J.M., Clack, T., Quail, P.H., and Sharrock, R.A. (1998). Coordination of phytochrome levels in phyB mutants of *Arabidopsis* as revealed by apoprotein-specific monoclonal antibodies. *Genetics* **149**, 523–535.
- Ishige, F., Takaichi, M., Foster, R., Chua, N.-H., and Oeda, K. (1999). A G-box motif (GCCACGTGCC) tetramer confers high-level constitutive expression in dicot and monocot plants. *Plant J.* **18**, 443–448.
- Kendrick, R.E., and Kronenberg, G.H.M., eds (1994). *Photomorphogenesis in Higher Plants*. (Dordrecht, The Netherlands: Kluwer Academic Publishers).
- Kim, L., Kircher, S., Toth, R., Adam, E., Schäfer, E., and Nagy, F. (2000). Light induced nuclear import of phytochrome-A:GFP fusion proteins is differentially regulated in transgenic tobacco and *Arabidopsis*. *Plant J.* **22**, 125–133.
- Kircher, S., Kozma-Bognar, L., Kim, L., Adam, E., Harter, K., Schäfer, E., and Nagy, F. (1999). Light quality-dependent nuclear import of the plant photoreceptors phytochrome A and B. *Plant Cell* **11**, 1445–1456.

- Koncz, C., Martini, N., Szabados, L., Hrouda, M., Bachmair, A., and Schell, J.** (1994). Specialized vectors for gene tagging and expression studies. In *Plant Molecular Biology Manual*, B.S. Gelvin and R.A. Schilperoort, eds (Dordrecht, The Netherlands: Kluwer Academic Press), pp. 1–22.
- Koornneef, M., Rolff, E., and Spruit, C.J.P.** (1980). Genetic control of light-inhibited hypocotyl elongation in *Arabidopsis thaliana* (L.) Heynh. *Z. Pflanzenphysiol.* **100**, 147–160.
- Martinez-Garcia, J.F., Huq, E., and Quail, P.H.** (2000). Direct targeting of light signals to a promoter element-bound transcription factor. *Science* **288**, 859–863.
- Menkens, A.E., Schindler, U., and Cashmore, A.R.** (1995). The G-box: A ubiquitous regulatory DNA element in plants bound by the GBF family of bZIP proteins. *Trends Biochem. Sci.* **20**, 506–510.
- Nagy, F., and Schäfer, E.** (2000). Nuclear and cytosolic events of light-induced, phytochrome-regulated signaling in higher plants. *EMBO J.* **19**, 157–163.
- Ni, M., Tepperman, J.M., and Quail, P.H.** (1998). PIF3, a phytochrome interacting factor necessary for normal photoinduced signal transduction, is a novel basic helix-loop-helix protein. *Cell* **95**, 657–667.
- Ni, M., Tepperman, J.M., and Quail, P.H.** (1999). Binding of phytochrome B to its nuclear signalling partner PIF3 is reversibly induced by light. *Nature* **400**, 781–784.
- Osterlund, M.T., Hardtke, C.S., Wei, N., and Deng, X.W.** (2000). Targeted destabilization of HY5 during light-regulated development of *Arabidopsis*. *Nature* **405**, 462–466.
- Oyama, T., Shimura, Y., and Okada, K.** (1997). The *Arabidopsis* HY5 gene encodes a bZIP protein that regulates stimulus-induced development of root and hypocotyl. *Genes Dev.* **11**, 2983–2995.
- Popov, N., Schmitt, M., Schulzeck, S., and Matthies, H.** (1975). Eine störungsfreie Mikromethode zur Bestimmung des Proteingehaltes in Gewebehomogenaten. *Acta Biol. Med. Germ.* **34**, 1441–1446.
- Poppe, C., and Schäfer, E.** (1997). Seed germination of *Arabidopsis thaliana* phyA/phyB double mutants is under phytochrome control. *Plant Physiol.* **114**, 1487–1492.
- Robson, P.R.H., Whitelam, G.C., and Smith, H.** (1993). Selected components of the shade avoidance syndrome are displayed in a normal manner in mutants of *Arabidopsis thaliana* and *Brassica rapa* deficient in phytochrome B. *Plant Physiol.* **102**, 1179–1184.
- Sakamoto, K., and Nagatani, A.** (1996). Nuclear localization activity of phytochrome B. *Plant J.* **10**, 859–868.
- Sambrook, J., Fritsch, F.E., and Maniatis, T.** (1989). *Molecular Cloning: A Laboratory Manual*. (Cold Spring Harbor, NY: Cold Spring Harbor Laboratory Press).
- Schaffer, R., Ramsay, N., Samach, A., Corden, S., Putterill, J., Carre, I.A., and Coupland, G.** (1998). The late elongated hypocotyl mutation of *Arabidopsis* disrupts circadian rhythms and the photoperiodic control of flowering. *Cell* **93**, 1219–1229.
- Sharrock, R.A., and Quail, P.H.** (1989). Novel phytochrome sequences in *Arabidopsis thaliana*: Structure, evolution, and differential expression of a plant regulatory photoreceptor family. *Genes Dev.* **3**, 695–707.
- Shinomura, T., Nagatani, A., Hanzawa, H., Kuboty, M., Watanabe, M., and Furuya, M.** (1996). Action spectra for phytochrome A- and B-specific photoinduction of seed germination in *Arabidopsis thaliana*. *Proc. Natl. Acad. Sci. USA* **93**, 8129–8133.
- Somers, D.E., Devlin, P.F., and Kay, S.A.** (1998). Phytochromes and cryptochromes in the entrainment of the *Arabidopsis* circadian clock. *Science* **282**, 1488–1490.
- Wagner, D., and Quail, P.H.** (1995). Mutational analysis of phytochrome B identifies a small COOH-terminal-domain region critical for regulatory activity. *Proc. Natl. Acad. Sci. USA* **92**, 8596–8600.
- Wang, H., Ma, L.-G., Li, J.-M., Zhao, H.-Y., and Deng, X.-W.** (2001). Direct interaction of *Arabidopsis* cryptochromes with COP1 in light control development. *Science* **294**, 154–158.
- Wang, Z.-Y., Kenigsbuch, D., Sun, L., Harel, E., Ong, M.S., and Tobin, E.M.** (1997). A Myb-related transcription factor is involved in the phytochrome regulation of an *Arabidopsis* *Lhcb* gene. *Plant Cell* **9**, 491–507.
- Wang, Z.-Y., and Tobin, E.M.** (1998). Constitutive expression of the CIRCADIAN CLOCK ASSOCIATED 1 (CCA1) gene disrupts circadian rhythms and suppresses its own expression. *Cell* **93**, 1207–1217.
- Whitelam, G.C., and Devlin, P.F.** (1997). Roles of different phytochromes in *Arabidopsis* development. *Plant Cell Environ.* **20**, 752–758.
- Yamaguchi, R., Nakamura, M., Mochizuki, N., Kay, S.A., and Nagatani, A.** (1999). Light-dependent translocation of a phytochrome B:GFP fusion protein to the nucleus in transgenic *Arabidopsis*. *J. Cell Biol.* **145**, 437–445.